International Conference on Space Optics—ICSO 2014

La Caleta, Tenerife, Canary Islands

7–10 October 2014

Edited by Zoran Sodnik, Bruno Cugny, and Nikos Karafolas

Recent progress in the development of MCT hot detectors

R. Wollrab

W. Schirmacher

T. Schallenberg

H. Lutz

et al.

esa icso proceedings cnes

International Conference on Space Optics — ICSO 2014, edited by Zoran Sodnik, Nikos Karafolas, Bruno Cugny, Proc. of SPIE Vol. 10563, 105632F · © 2014 ESA and CNES
CCC code: 0277-786X/17/$18 · doi: 10.1117/12.2304268

RECENT PROGRESS IN THE DEVELOPMENT OF MCT HOT DETECTORS

R. Wollrab, W. Schirmacher, T. Schallenberg, H. Lutz, J. Wendler, M. Haiml, J. Ziegler
AIM INFRAROT-MODULE GmbH, Theresienstr. 2, D-74072 Heilbronn, Germany

ABSTRACT

To push HOT-performance, AIMs existing n-on-p technology has been improved by introducing Gold as an acceptor and reducing its concentration to the lower $10^{15}/cm^3$ range as well as by optimizing the passivation process. This results in a substantial reduction in dark current density, a prerequisite for HOT operation. Recent dark current data are compared to ones previously obtained as well as to Tennant`s Rule07 [1], a generally accepted bench mark in this context.
Furthermore, we present electro-optical parameters obtained in the temperature range from 120 K to 170 K on resulting FPAs with 640x512 pixels, a pitch of 15 µm and a typical (80 K) cutoff wavelength of 5.1 µm.

I. INTRODUCTION

Evolving markets for small and micro-satellites drive the demand for systems with minimal size, weight and power (SWaP). Focal plane arrays (FPAs), especially designed for high operating temperatures (HOT) detectors are a key of this development, because they can be operated with a smaller, light weight and power saving cooling engine, the otherwise dominant component.
Such HOT MWIR-detectors are typically meant to be operated at 150 K and beyond while preserving performance characteristics formerly only obtained at substantially lower temperatures (typ. 80 K to 100 K). In this respect, Mercury Cadmium Telluride (MCT) presents distinct advantages over competing material systems as its band gap can be perfectly tuned to the desired spectral sensitivity and operating temperature.

II. TECHNOLOGICAL ASPECTS

The manufacturing of MCT-based photovoltaic (pv) detectors at AIM is made along two tracks: One is the well established process on epitaxial MCT-layers grown by liquid phase epitaxy on CdZnTe substrates. The other track relies on molecular beam epitaxy (MBE) using 4-inch GaAs substrates [2, 3]. The HOT-detectors considered here are LPE-based.
A dislocation density smaller than $1x10^5$ cm^{-2}, revealed as etch pit density (EPD) on the epilayer by an adequate etching process, has been identified as a crucial factor for optimum detector performance [4]. Here, the EPD of the CdZnTe substrates, as determined by Nakagawa-etching, is kept below $5x10^4$ cm^{-2}. The EPD of the epitaxial layers regularly reproduces the substrate EPD.
The p-type doping of the epitaxial layer is done by gold while the number of Hg-vacancies, well known to be connected with a Shockley-Read (SR) recombination center [5], is kept low.
The surface of the epilayers is submitted to a sequence of dedicated cleaning and etching processes to ensure a highly clean surface. A CdTe passivation layer is deposited on top of it. A strong interdiffusion with the underlying MCT is then created by a newly developed process. The resulting Cd-profile, as determined by secondary mass spectroscopy (SIMS), is shown in Fig. 1.
This profile translates into a continuous increase of the bandgap towards the surface on a distance of approximately 800 nm. The resulting electric field makes sure that minority carriers are repelled from remaining defects like impurities or lattice imperfections located at the surface, thereby suppressing related recombination processes. Applying this step in an optimized manner proved to be an essential measure for lowering the dark current density, as will be shown in section III.
The remaining steps are done by applying AIM's standard processing techniques, which have been refined over several years. The isolated n-type regions are created by implantation of boron. n- and p-contacts are made by depositing appropriate metals. After wafer dicing, the MCT chips are hybridized by flip chip bonding with either a Si based read out integrated circuit (ROIC) or a fan-out circuit consisting solely of metal wiring and allowing direct access to the diodes. The contact between MCT chips and their Si-counterparts is established by indium spheres, which are created by a reflow process. Finally the CdZnTe is removed from the MCT chips and an antireflection coating is deposited on top of it. The chosen FPA design contains 640x512 pixels with a pixel pitch of 15 µm, a well established and mature product line at AIM.

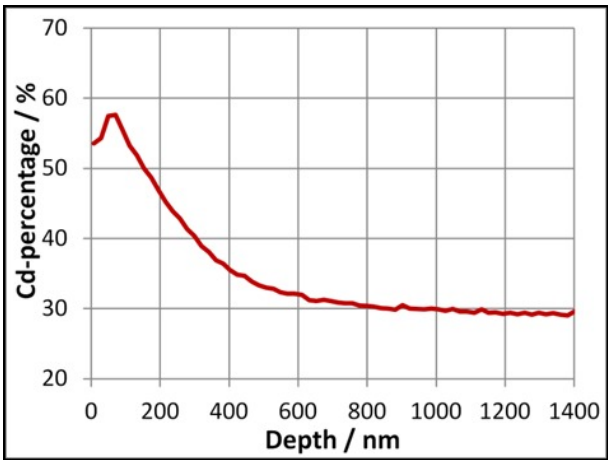

Fig. 1. SIMS profile of the Cd-percentage of a MWIR-LPE layer after application of a customized passivation process for HOT-operation. After deposition of CdTe, an appropriate annealing step is applied to strongly interdiffuse the two layers.

III. CHARACTERIZATION

Dark current measurements are performed on MCT-chips hybridized to fan-out circuits (fanouts). On these fanouts several photodiodes are connected in parallel allowing the measurement of the expected low currents. The diode fields are square shaped, the size being given by the number of pixels along the edges. Those diode fields are surrounded by rows of interconnected diodes around the perimeter that can be independently biased and thus act as guard structures. In that way, current generated outside the pixel field under consideration is effectively siphoned off. The measurements are performed in a custom made liquid nitrogen evaporation cryostat where the temperature can be varied and stabilized between 80 K and 300 K. For dark current evaluation, the fanouts are mounted into a closed cavity held at detector temperature.
A number of data points from dark current measurements are displayed in Fig. 2. These data were obtained during the last two years from several different fanouts where the doping level of the p-type absorber had been varied. In order to eliminate variations due to cutoff wavelength λ_{CO} and operating temperature T_{OP}, the data have been divided by the predictions of the so called Rule07. This rule, first presented by Tennant [1] in 2007, is based on a multitude of data from Teledyne´s detectors and predicts dark current density as a function of λ_{CO} and T_{OP}.

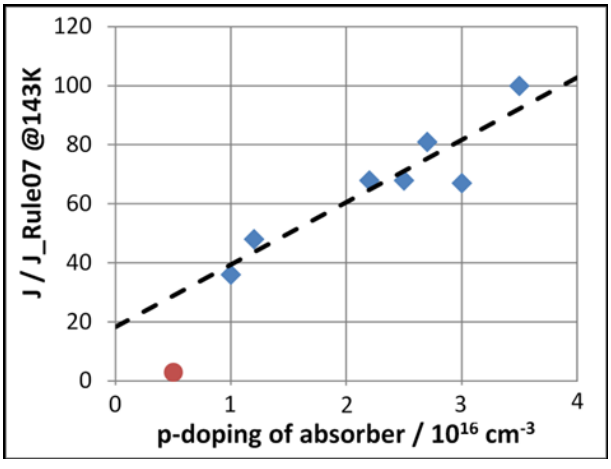

Fig. 2. Comparison of dark current densities of several MWIR detectors taken over the course of the last two years. The diamond-shaped data points stem from detectors without the improved passivation process. The ball-shaped point corresponds to our latest HOT-technology where the improved passivation process was applied.

Two groups of data points can be distinguished in Fig. 2: The blue, diamond-shaped ones correspond to detectors with varied absorber doping levels but without applying the optimized passivation process. The red, ball-shaped data point originates from the most recently developed detector on which we applied the improved passivation process as depicted by Fig. 1.
The diamond-shaped data points seem to follow a linear relationship fairly well. The data implies that a reduction of the absorber doping level seems to be a necessary step to reduce the dark current.
However, extrapolating the data to doping levels below $1 \cdot 10^{16}$ cm^{-3} shows that this strategy alone would not get the dark current down to the level described by Rule07, which corresponds to a value of 1 in this graph. The ball-shaped data point significantly deviates from the linear fit. This indicates that lowering the doping level to $5 \cdot 10^{15}$ cm^{-3} in combination with an improved passivation process is a decisive step to get closer to Rule07.
In Fig. 3 the dark current levels of two different detectors are compared with the Rule07. The green data points are taken from a measurement that was done about two years ago with a standard MWIR-detector, while the red data represents the latest HOT design. Both detectors had slightly different λ_{CO}, but the data have been converted to λ_{CO} = 5.20 µm, which was also used for the calculation of the depicted Rule07. The data show a significant decrease of the dark current density obtained by lowering the doping level as well as applying the improved passivation process. At an operating temperature of 165 K, the dark current density of the HOT-device exceeds the prediction of Rule07 by just a factor of two. Because the improved passivation process still offers some potential for optimization and it also seems reasonable to decrease the p-doping level further, we think that reaching or even going below the Rule07 seems well possible at this point.
The measures taken to lower the dark current apparently also diminished the tunneling current at higher bias. Fig. 4 and Fig. 5 compare the current-voltage (IV) characteristics taken at temperatures between 111 K and 166 K of two detectors manufactured with different sets of technological parameters.
Fig. 4 shows data from a detector with slightly improved technology measured in early 2013, while Fig. 5 corresponds to the most recent HOT-technology (end of 2013). The IV-curves of the previous technology show a distinct tunneling behavior, which dominates the current at lower temperatures and higher bias.

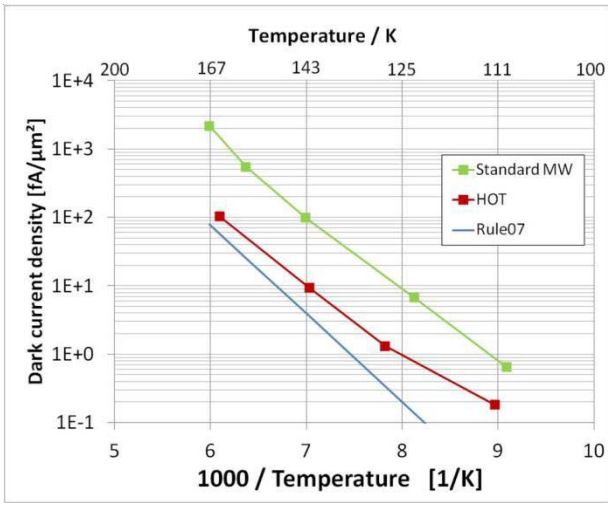

Fig. 3. Comparison of the dark current density of two different detector technologies with the predictions of the Rule07. The green symbols correspond to the standard AIM technology, measured two years ago. The red data points are from a recent HOT-device. The detectors have slightly different cutoff wavelengths and the data have all been converted to 5.2 µm at 77 K.

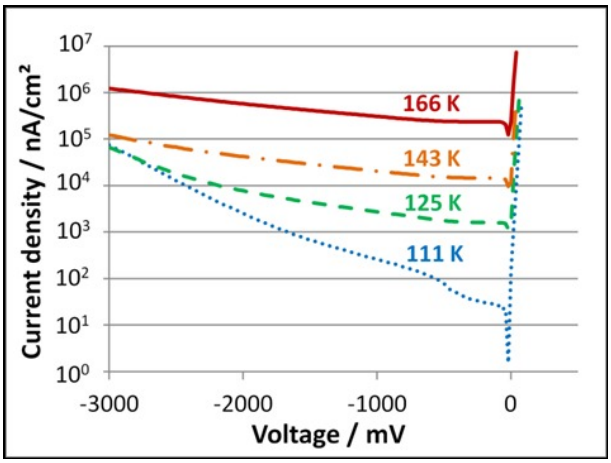

Fig. 4. Dark IV-characteristics of a MWIR detector array with a cutoff wavelength of 5.3 µm at 77 K, measured at four different temperatures. This detector was fabricated in early 2013 with a modified standard technology. Note the tunneling at lower temperatures.

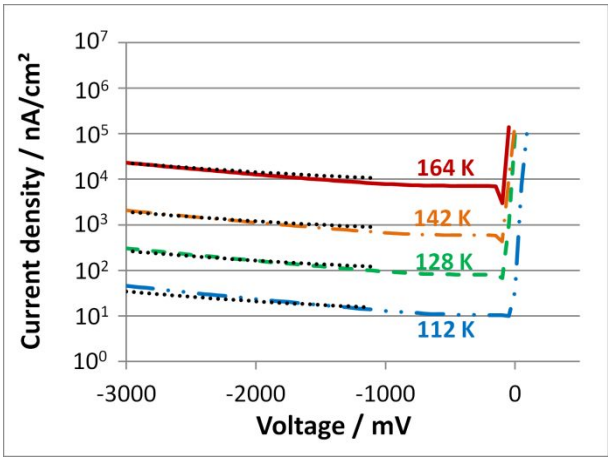

Fig. 5. Dark IV-characteristics of a MWIR detector array with a cutoff wavelength of 5.1 µm at 77 K, measured at four different temperatures. This detector was fabricated in autumn 2013 using the most recent HOT technology. The detector appears to be limited by avalanche multiplication at larger reverse bias as indicated by the close match to Beck`s model (dotted lines).

On the other hand, the data of our most advanced HOT-technology shows very little increase of the current between a typical operating bias of -200 mV and the maximum voltage of –3000 mV. Tentatively these characteristics can be compared to an empirical model describing avalanche multiplication first formulated by Beck [6] for MWIR and LWIR diodes, see (1) and (2).

$$M = 1 + 2^{\frac{2(V - V_{th})}{V_{th}}} \tag{1}$$

$$V_{th} = 6.8\, E_g / e \tag{2}$$

Taking the current density measured at -200 mV as a basis (M = 1) and then applying (2), one obtains the estimated values as depicted by the dotted black lines in Fig. 5. For voltages < -1000 mV the match to the experimental values is deemed excellent. We therefore conclude that in the considered temperature and voltage range, avalanche multiplication is the limiting process for the present HOT-technology and that tunneling does not play a significant role.

III. FPA

For further investigation, detectors fabricated in the current HOT-technology have been hybridized with ROICs to form FPAs and integrated in a suitable dewar combined with a Stirling engine allowing to vary the FPA temperature between 80 and 200 K. A cold shield kept at detector temperature limits the aperture to an F-number of 3.5. The dewar cover is sealed by an entrance window designed as an optical band-pass with an upper limit larger than the detector cut-off wavelength. The detector considered here has 640x512 pixels with a pitch of 15 µm in both x- and y-direction. The cutoff wavelength measured at 80 K is 5.1 µm.
The signal under illumination is determined by placing the detector in front of a large area 300 K blackbody. The integration time is adjusted in such a way as to achieve a half well filling of the integration capacitor (holding up to $6 \cdot 10^6$ electrons). From this measurement the total (photo + dark) current density is calculated. Temperature dependent values averaged over the entire matrix are shown in Fig. 6 as red squares.
To evaluate the dark signal, the detector is pointed at a black target cooled to liquid nitrogen temperature. Under these conditions, some residual light can reach the detector. The resulting parasitic signal (insignificant for temperatures > 150 K) is computed from the asymptotic value seen at the lowest temperatures and then subtracted from the measured data. Mean dark current densities so obtained are shown in Fig. 5 as green triangles.
The difference between total and dark current density gives the photocurrent density shown as blue diamonds in Fig. 6. Its decreasing slope reflects the shift of cutoff wavelength with temperature. The crossover of dark and photocurrent, which is indicative of the maximum sensible operating temperature, is found at 175 K under the aforementioned conditions.
The noise equivalent temperature difference (NETD), as an important figure of merit for the performance of detectors, is also determined under the same conditions. In Fig. 7, the temperature dependent average values for this array are shown as blue diamonds. Up to a temperature of 150 K, only a slight increase can be observed for the current technology. This compares very favorably with standard technology (red squares) or previous HOT results from early 2013 (green triangles).
First infrared images taken with this module at FPA temperatures of 140, 160 and 170 K in a laboratory setup are shown in Fig. 8. Excellent thermal resolution and contrast are obtained up to 160 K. At 170 K the influence of increasing dark current starts to become performance limiting in this configuration.

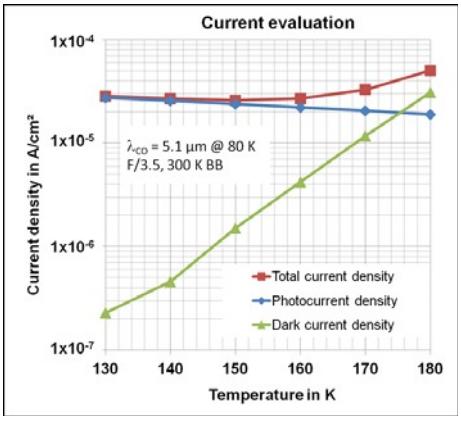

Fig. 6. Mean current densities evaluated on an FPA with 640x512 pixels in a 15 µm pitch and a cut-off wavelength of 5.1 µm at 80 K. The total current (red squares) is determined for a 300 K blackbody illumination with a field of view corresponding to an F-number of 3.5. Dark current (green triangles) has been corrected for a residual photo signal determined from an asymptotic value at low temperature. Photocurrent density (blue diamonds) results from the difference between total and dark current densities.

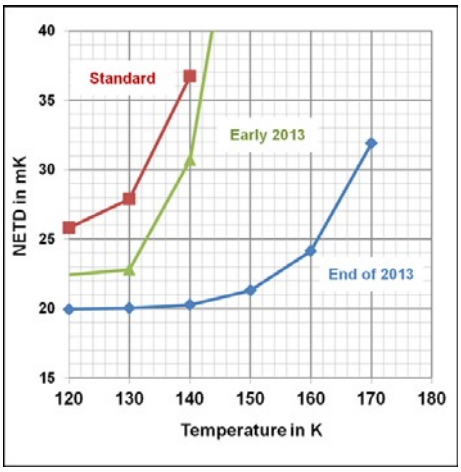

Fig. 7. Comparison of NETD(T) of three different MWIR detector arrays. The standard-detector (red, squares) has a cutoff wavelength at 80 K of 5.2 µm, the HOT detector from early 2013 (green, triangles) of 5.3 µm, and the HOT-detector from end of 2013 (blue, diamonds) of 5.1 µm.

Fig. 8. Infrared images taken with an F/3.5 optics at FPA temperatures of 140, 160, and 170 K with a HOT detector fabricated in the most recent technology (end of 2013). The detector has a 640x512 pixel format with 15 µm pitch and a cut-off wavelength of 4.75 µm at 160 K.

III. CONCLUSION

We have shown that a lower p-type doping level of the absorber is connected with decreased dark current levels in a linear manner. Improving the passivation process shifts those levels to even lower values and appears to be a crucial step for our technology to close in on the performance predicted by the Rule07. With the present HOT technology, the dark current density at 165 K is two times that prediction. Since the improved passivation technology is not yet fully optimized, a further decrease of the dark current density seems to be within reach. In addition, the tunneling currents of the photodiodes have been significantly reduced and the IVcharacteristics

appear to be limited by avalanche multiplication up to a reverse bias of 3 V, in good agreement with Beck's empirical model. The introduced improvements also lead to a better NETD(T) characteristic that remains essentially flat up to 150 K. Excellent infrared images in terms of thermal resolution and contrast have been obtained in a laboratory setup at an FPAtemperature of 160 K. Further optimization of passivation and doping parameters is expected to entail even higher operating temperatures in the near future.

REFERENCES

[1] W. E. Tennant, D. Lee, M. Zandian, E. Piquette, M. Carmody, *J. Electron. Mater.* **37**, pp. 1406, (2008)
[2] J. Wenisch, D. Eich, H. Lutz, T. Schallenberg, R. Wollrab, J. Ziegler, *J. Electron. Mater.* **41**, pp. 2828, (2012)
[3] J. Wenisch, H. Bitterlich, M. Bruder, P. Fries, R. Wollrab, J. Wendler, R. Breiter, J. Ziegler, *J. Electron. Mater.* **42**, pp. 3186, (2013)
[4] H. Figgemeier, M. Bruder, K.-M. Mahlein, R. Wollrab, J. Ziegler, *J. Electron. Mater.* **32**, pp. 588, (2003)
[5] M. A. Kinch, F. Aqariden, D. Chandra, P.-K. Liao, H. F. Schaake, H. D. Shih, *J. Electron. Mater.* **34**, pp. 880, (2005)
[6] M. A. Kinch, J. D. Beck, C.-F. Wan, F. Ma, J. Campbell, *J. Electron. Mater.* **33**, pp. 630, (2004)